sustainability

MDPI

Article

Comparative Assessment of Palmer Drought Indices for Hydrological and Agricultural Drought in the Mediterranean Ceyhan Basin, Türkiye

Mehmet Dikici [1,*], Kürşat Şekerci [2], Yasin Paşa [3] and Mehmet Ali Çelik [4,5]

[1] Department of Civil Engineering, Alanya Alaaddin Keykubat University, Alanya 07425, Türkiye
[2] Department of Civil Engineering, Bingol University, Bingol 12000, Türkiye; ksekercii@bingol.edu.tr
[3] Department of Civil Engineering, İstanbul Gelişim University, Istanbul 34310, Türkiye; ypasa@gelisim.edu.tr
[4] Geography Department, Faculty of Arts and Sciences, Igdir University, Igdir 76000, Türkiye; mali.celik@igdir.edu.tr
[5] Department of Geography, Nakhchivan State University, AZ 7012 Nakhchivan, Azerbaijan
* Correspondence: mehmet.dikici@alanya.edu.tr

Abstract

Hydrological drought is an increasing challenge for water security, ecosystem resilience, and water resource management in Mediterranean river basins, emphasizing the need for reliable indicators capable of capturing regional hydroclimatic variability. This study evaluates the effectiveness of the Palmer Hydrological Drought Index (PHDI) and its self-calibrating version (scPHDI) for hydrological drought assessment in the Ceyhan Basin, Türkiye. A homogenized long-term dataset of meteorological and streamflow records (1970–2024) was developed, with missing climatic data reconstructed using PRISM-based spatial interpolation, and complemented by groundwater records (2002–2015). Monthly Palmer indices were calculated using a soil water balance approach at individual stations and aggregated to the basin scale through weighted averaging. The indices were compared with SPI12 and SPEI12, which share the same meteorological forcing, and with the streamflow-based SRI12, alongside spatial and temporal analyses of drought occurrence. The results reveal a clear intensification of drought conditions after the early 2000s, with increasing frequencies of moderate and severe drought events across the basin. The self-calibrating Palmer hydrological index showed improved spatial consistency by adapting index parameters to local climatic characteristics. Agreement between scPHDI and the streamflow-based SRI12 supported the hydrological relevance of the detected drought signal, whereas agreement with SPI12 and SPEI12 was interpreted as a benchmark rather than as independent validation. The findings indicate that scPHDI is a promising indicator for retrospective hydrological drought assessment and may contribute to drought monitoring systems in Mediterranean basins, although its forecasting skill and warning lead time remain to be demonstrated.

Keywords: Palmer Drought Severity Index; drought monitoring; Mediterranean Basin; water resources management; Ceyhan Basin

Check for updates

Academic Editor: Xuchao Zhu

Received: 25 August 2026
Revised: 21 October 2026
Accepted: 21 October 2026
Published: 24 October 2026

Copyright: © 2026 by the authors. Licensee MDPI, Basel, Switzerland. This article is an open access article distributed under the terms and conditions of the Creative Commons Attribution (CC BY) license.

1. Introduction

Within contemporary efforts to plan, develop, and manage water resource in areas negatively affected by climate change, the mitigation of expected drought impacts has become highly important [1,2]. Managing the increasing risk of drought and achieving

adaptation to this risk require the development of sustainable and effective drought risk management strategies that adopt holistic (integrated) approaches [3,4]. In semi-arid and Mediterranean agricultural regions where irrigation relies heavily on aquifers and surface-water supply is limited or irregular, the impacts of drought can be exacerbated by excessive groundwater abstraction, which lowers water tables, reduces baseflow to rivers, and diminishes the buffering capacity of aquifers during dry periods [5–7]. These conditions highlight the increasing importance of integrated basin-scale management as a proactive strategy for drought mitigation and adaptation [6]. Drought management is part of disaster management [8]. Drought Risk Management refers to the concept and practice of preventing and reducing the adverse consequences and potential disaster effects of drought hazards through protection, mitigation, and preparedness activities and measures [9,10]. Drought risk management constitutes an important component of water resources management policies and strategies. National drought policies play a major role in managing drought risk [3]. To reduce the impacts of drought, drought management plans must be prepared on the basis of national legislation and taking into account the basin's specific drought characteristics and impacts [11]. For these plans to achieve coherence, it is important that they be prepared as part of an integrated basin management plan. In addition, involving all stakeholders, affected sectors, decision makers, and experts during plan development substantially contributes to the success of drought-management plans.

Elements of a drought management plan include knowledge of the river basin characteristics, review of historical drought events in the basin, risk assessment, selection of indicators and threshold values for drought analysis, development of a mitigation program to reduce drought impacts, and establishment of an early warning system and organizational structure [12]. Drought risk management covers hazard and exposure assessment, impact and vulnerability assessment, drought monitoring and forecasting as part of an early warning system, preparedness, and mitigation [8]. Early-warning systems are one of the most important elements of drought-management plans and are used with two primary objectives: drought monitoring and drought forecasting. Drought early warning systems typically aim to monitor, evaluate, and present information on climate, hydrological characteristics, water supply conditions, and trends. The purpose is to provide information sufficiently early, before or during the onset of drought, to enable action under a drought risk management plan to reduce potential impacts [13].

Drought is a slowly evolving hydroclimatic phenomenon that develops gradually over time, making continuous monitoring and assessment essential for effective risk management and mitigation [14]. A wide range of drought indicators and indices has been developed to quantify different characteristics of drought, including its severity, spatial extent, duration, onset, and temporal evolution. These metrics facilitate the identification, classification, and monitoring of drought events across diverse climatic and environmental conditions. In addition, several drought indicators serve as valuable tools for validating model simulations, remotely sensed drought products, and datasets generated through the assimilation of remote sensing observations into modeling frameworks [13]. Broadly, current drought monitoring and early-warning systems are based on three methodological approaches: (i) the application of a single drought indicator or index, (ii) the integration of multiple drought indicators or indices to capture complementary aspects of drought dynamics, and (iii) the use of combined or hybrid indicators that merge different sources of information to improve the reliability and comprehensiveness of drought assessment.

According to the World Meteorological Organization (WMO) Integrated Drought Management Programme (IDMP), developed in collaboration with the Global Water Partnership (GWP), drought indicators and indices are classified into five principal categories based on their underlying characteristics: meteorological, soil moisture, hydrological, remote

sensing, and composite or model-based indicators [13]. The selection of an appropriate indicator or index depends primarily on the availability of data, the spatial and temporal scale of analysis, and the specific objectives of the assessment [13,15]. Indicators derived from precipitation records are generally used to characterize meteorological drought, whereas other indices are specifically designed to assess hydrological or agricultural drought, soil moisture deficits, or water shortages affecting urban water supply systems [16,17]. Consequently, the choice of drought indicator should be aligned with the drought type under investigation and the intended application to ensure reliable and meaningful assessment outcomes. A variety of drought indices are used internationally to characterize drought (severity, frequency, and duration) [17,18]. Basin hydroclimatic conditions and physical characteristics affect the performance of drought indices [19,20]. Numerical index values are critical for appropriately and accurately assessing drought severity, operating drought early warning systems, and informing comprehensive drought planning [13].

Among the soil-moisture-based indicators, the Palmer Drought Severity Index (PDSI) is one of the most widely used [18,21]. It is derived from a two-layer soil water balance driven by monthly precipitation, temperature, and the available water holding capacity (AWHC) of the soil, and it expresses the departure of the actual moisture supply from the climatically appropriate supply for existing conditions (CAFEC) as a standardized, dimensionless value [21,22]. The Palmer Hydrological Drought Index (PHDI) uses the same water balance but a stricter criterion for the termination of dry and wet spells, which makes it more representative of slowly responding storages such as streamflow, reservoirs, and groundwater [17,18]. Compared with precipitation-only indices such as the SPI [23], the Palmer indices explicitly account for evaporative demand, soil water storage, and the persistence of moisture anomalies, and therefore provide a more physically based representation of agricultural and hydrological drought [13,24]. Their main weaknesses, empirical constants derived for the central United States and limited spatial comparability [15,22], were addressed in part by the self-calibrating Palmer Hydrological Drought Index (scPHDI), which adjusts the relevant index parameters to local climatic conditions using the available observational record [25,26]. These properties make the Palmer family a suitable candidate for basins with a strongly seasonal water balance and a marked summer moisture deficit, such as the Mediterranean Ceyhan Basin.

Although numerous drought indices have been developed to monitor hydroclimatic variability across different spatial and temporal scales, selecting the most appropriate index remains a major challenge because their performance varies with climatic conditions, data availability, and the specific type of drought being assessed [16,19]. In the Ceyhan Basin, and in comparable Mediterranean catchments more broadly, previous studies have predominantly relied on conventional single-index approaches [27–31] or have cross-compared drought metrics that share the same underlying meteorological forcing, offering only circular confirmation of drought signals rather than genuine physical validation. Comparative assessments that jointly evaluate the original Palmer indices and their self-calibrating variants while validating their outputs against truly independent, non-climatic evidence remain scarce, leaving an unresolved question of whether Palmer-based indices can reliably capture drought impacts that manifest beyond the atmosphere, in streamflow regimes, agricultural land use and production, and groundwater systems. This represents an important knowledge gap for Mediterranean environments, where agricultural and hydrological droughts exhibit complex spatial and temporal dynamics [14,32].

Addressing this gap, the present study reconstructs a homogenized long-term gridded dataset (1970–2024) using PRISM-based spatial interpolation and systematically compares PDSI, PHDI, and scPHDI at both station and basin scales. The proposed framework introduces a dual-validation approach that extends beyond simple index comparison:

Palmer-based indices are first cross-compared against multi-scalar meteorological benchmarks (SPI12 and SPEI12) to evaluate temporal lag and water-balance sensitivity under identical climate forcing and are then compared with non-meteorological evidence, namely streamflow records (SRI12), cultivated area, and production statistics for wheat and cotton, and recorded groundwater table decline. By combining dynamic water-balance indices with independent hydro-agricultural ground-truth validation, this study provides a framework for retrospective drought monitoring in Mediterranean basins that can inform the future design of drought early-warning systems.

2. Data and Methods

For the drought analysis of the Ceyhan Basin, data gap analyses were conducted for meteorological, hydrological, and hydrogeological datasets to evaluate data availability. Based on this evaluation, 1970–2024 was adopted as the longest common period for meteorological and streamflow data, whereas agricultural and groundwater records were available only for 2002–2015. Missing values were reconstructed with the methods described below to produce continuous time series. Meteorological, hydrological, and agro-hydrogeological data for the Ceyhan Basin were compiled and reconstructed through PRISM-based spatial interpolation to produce homogenized input series. These series were used to calculate the PHDI and its self-calibrating version (scPHDI) for hydrological drought assessment [33,34]. The resulting indices were compared with SPI12 [23] and SPEI12 [35], which share the same meteorological forcing, and with the streamflow-based SRI12 [36]. Station-based and basin-wide spatiotemporal analyses, together with Mann–Kendall trend analysis of natural streamflow, were then used to characterize drought occurrence patterns, which were linked to observed agricultural production and groundwater-abstraction data to assess drought impacts. The workflow concludes with recommendations for basin-scale drought risk management and early-warning threshold development (Figure 1).

2.1. Study Area and Meteorological Data

The Ceyhan Basin is located in southern Türkiye and drains from the Taurus Mountains in the north to the Mediterranean Sea in the south. It comprises the Upper, Middle and Lower Ceyhan sub-basins, whose boundaries, river network, reservoirs and meteorological stations are shown in Figure 2. Flows in the middle and lower parts of the basin are regulated by several large reservoirs, including Menzelet, Sır and Aslantaş, and the lower basin, located in the Çukurova region, is one of the main irrigated agricultural areas of Türkiye.

A large number of meteorological observation stations (MOS) have been established in and around the Ceyhan Basin. Some of these stations have long-term records, some have short records, and others have intermittent observations. Many stations are currently inactive.

Initially, available active and inactive stations were evaluated in terms of their representativeness of the basin and record length, and meteorological observation stations to be used in the drought analysis were selected.

Meteorological stations are generally irregularly distributed. Therefore, direct use of observation data from these stations in model-based climate research can lead to various problems. For this reason, observations from meteorological stations are commonly transferred to grid points. This is a necessary and important process because gridded datasets allow climatic variables to be well characterized even in regions distant from observation stations [37].

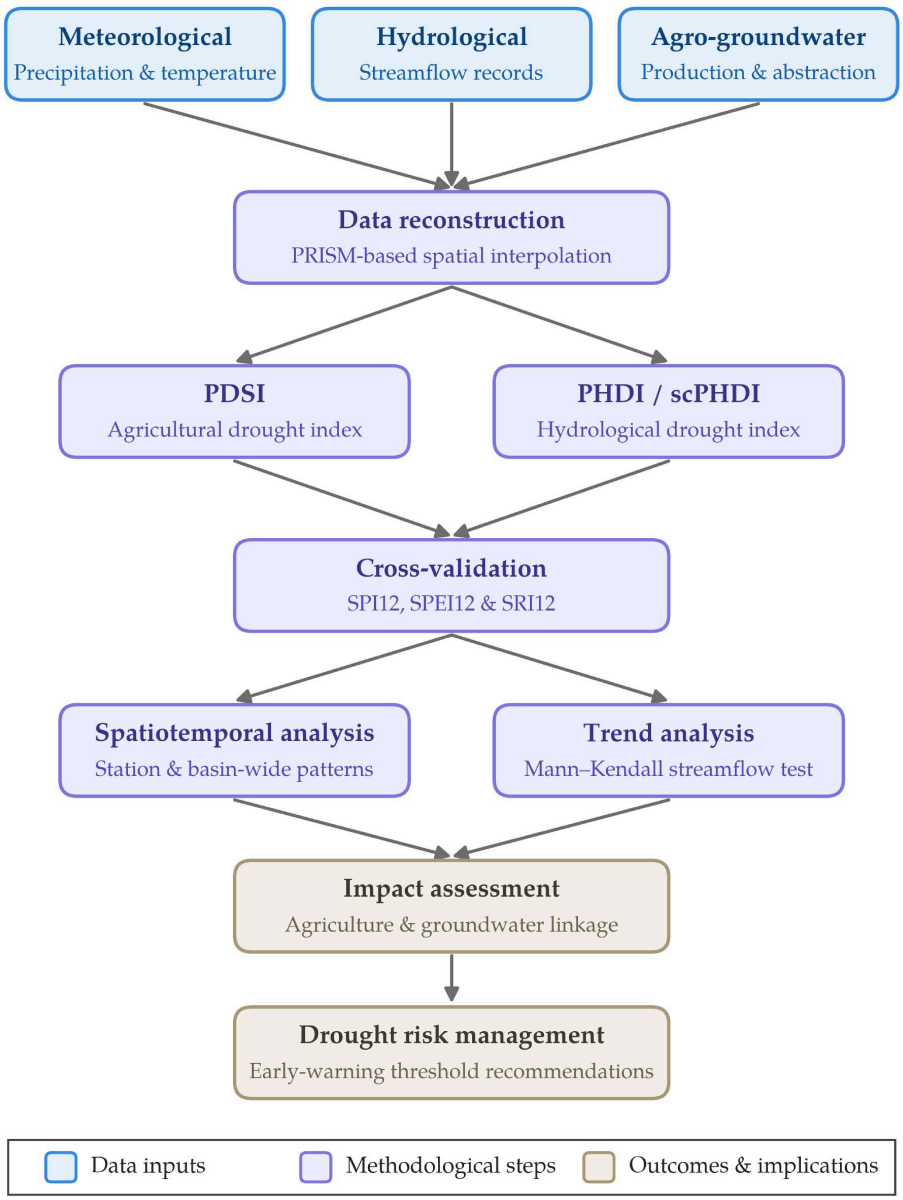


Figure 1. Schematic workflow of the study methodology.

Various methods are applied to transfer observation data to grid points. The PRISM model (Parameter-elevation Relationships on Independent Slopes Model), which accounts for the complex characteristics of the region in interpolation of observation data, is a good example [38]. When using the PRISM approach, appropriately weighting the stations to be interpolated to the target grid cell is crucial. In this way, stations are weighted based on their mutual distances, elevation, aspect, distance to the sea, and topographic attributes [39]. The length and continuity of hydrometeorological records are critically important for the accuracy and reliability of analysis outcomes. Accordingly, missing precipitation and temperature data for the meteorological stations selected for drought analysis were completed for the 1970–2024 period using the PRISM approach, which accounts for elevation, aspect, and maritime influence, and continuous time series were produced for analysis (Table 1a).

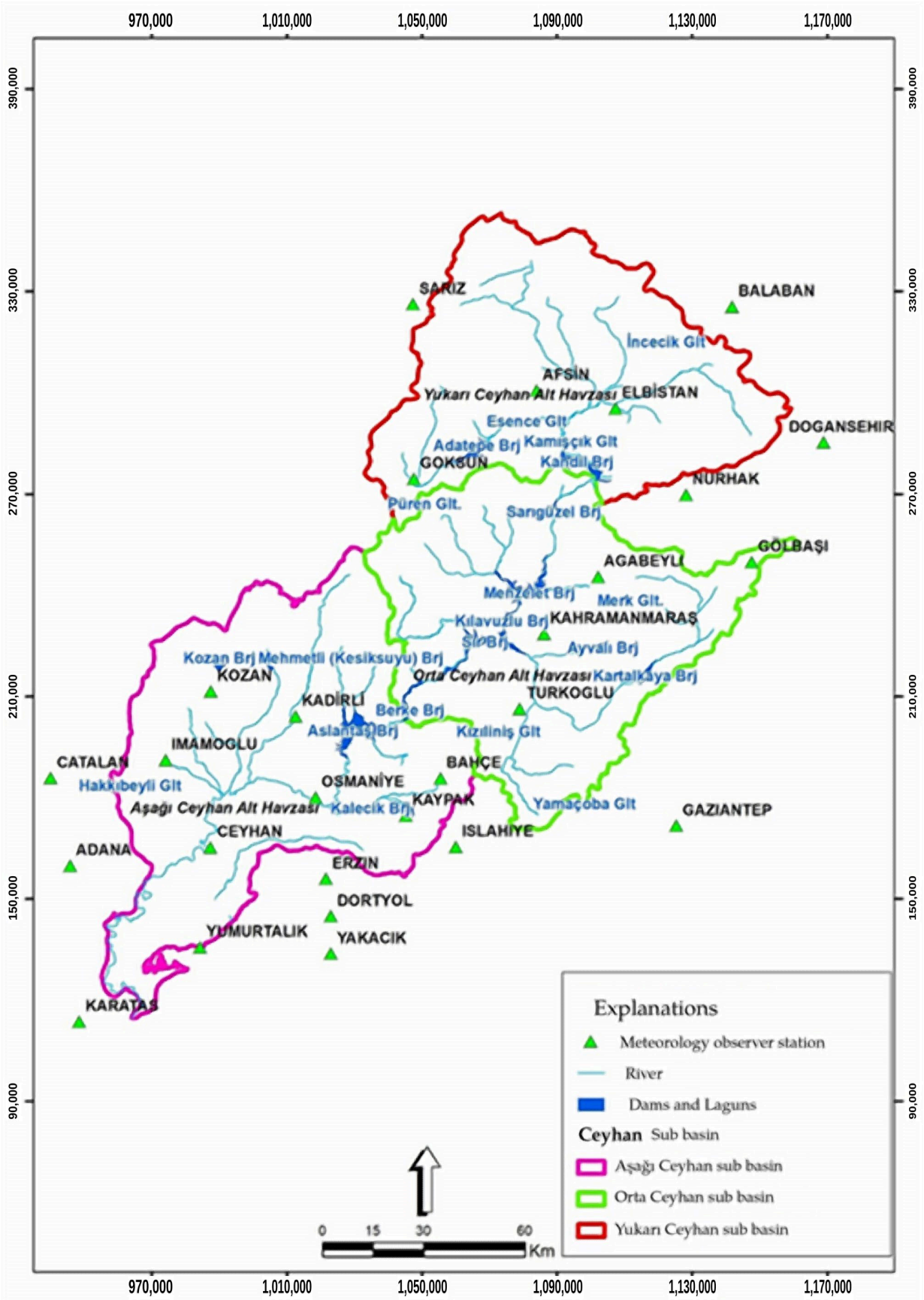


Figure 2. Meteorological observation stations in and around the Ceyhan Basin.

Table 1. (**a**). Summary of the reconstruction and validation performance for missing monthly precipitation and mean temperature records, including the number of stations, proportion of reconstructed records, validation method, coefficient of determination (R^2), root mean square error (RMSE), mean absolute error (MAE), and bias. (**b**). Leave-one-out reconstruction errors for monthly precipitation by season, station elevation, and dry months.

(**a**)

Variable	Number of Stations	Missing Records Reconstructed (%)	Validation Method	R^2	RMSE	MAE	Bias
Monthly precipitation	26	5.8	Leave-one-out cross-validation	0.95	14.8 mm	10.3 mm	0.7 mm
Monthly mean temperature	26	2.9	Leave-one-out cross-validation	0.99	0.58 °C	0.42 °C	0.03 °C

(**b**)

Group	RMSE (mm)	MAE (mm)	Bias (mm)	Relative RMSE (% of Mean)
Season				
Winter (DJF)	22.3	16.0	−0.8	23
Spring (MAM)	14.0	10.0	+0.5	25
Summer (JJA)	5.0	3.2	+1.8	50
Autumn (SON)	12.0	8.5	+1.0	30
Elevation				
<500 m	11.5	8.0	+0.3	21
500–1000 m	14.5	10.2	+0.6	24
>1000 m	19.0	13.5	+1.5	30
Dry months				
P < 25th percentile (all stations)	6.5	4.8	+2.1	55

Table 1b indicates that reconstruction errors vary across seasons and elevation classes. RMSE is highest in winter (22.3 mm) and at elevations above 1000 m (19.0 mm), suggesting greater uncertainty under wetter and more topographically variable conditions. In contrast, absolute errors are lowest during summer and dry months, although their relative RMSE values are higher (50% and 55%, respectively) because mean precipitation is low. Overall, the relatively small biases indicate limited systematic over- or underestimation.

Within the scope of the Ceyhan Basin drought analysis, data obtained from 15 Meteorological Observation Stations (MOS) located within the basin boundaries were utilized (Table 2).

Table 2. Meteorological observation stations within the Ceyhan Basin used in the drought analysis.

No	Station No	Name	Province	Latitude	Longitude	Elevation	Status
1	17,868	Afşin	Kahramanmaraş	38°15′	36°55′	1180	Open
2	7946	Bahçe	Osmaniye	37°13′	36°35′	665	Open
3	17,960	Ceyhan	Adana	37°02′	35°49′	30	Open
4	17,870	Elbistan	Kahramanmaraş	38°12′	37°11′	1137	Open
5	17,866	Göksun	Kahramanmaraş	38°01′	36°30′	1344	Open
6	17,871	Gölbaşı	Adıyaman	37°47′	37°38′	900	Open
7	7767	Kadirli	Osmaniye	37°23′	36°06′	100	Open
8	17,255	Kahramanmaraş	Kahramanmaraş	37°36′	36°56′	572	Open
9	17,908	Kozan	Adana	37°27′	35°49′	109	Open
10	17,355	Osmaniye	Osmaniye	37°10′	36°10′	120	Open
11	17,979	Yumurtalık	Adana	36°46′	35°47′	27	Open
12	7251	Ağabeyli	Kahramanmaraş	37°45′	37°07′	950	Closed
13	7937	İmamoğlu	Adana	37°16′	35°40′	100	Closed
14	8115	Kaypak	Osmaniye	37°07′	36°28′	700	Closed
15	7600	Türkoğlu	Kahramanmaraş	37°24′	36°51′	500	Closed

The locations of the Turkish State Meteorological Service (MGM) stations used in the drought analyses within the basin and its immediate surroundings are presented on the map in Figure 2.

Precipitation data from the meteorological stations located within the Ceyhan Basin were examined, and Figure 3 shows the aerial distribution of the stations' annual mean precipitation across the basin. Graphs of the monthly mean precipitation for the basin stations are presented in Figure 4. Examining the monthly total precipitation averages in the Ceyhan Basin reveals that winter and spring are the wet seasons, whereas the summer months and the beginning of autumn are dry. The driest month is August (6.7 mm), and the wettest month is December (100.4 mm). Considering the stations' long-term annual total precipitation averages, the highest mean precipitation (824.9 mm) was observed at the Kaypak station, while the lowest (390.7 mm) was recorded at the Elbistan station. The long-term annual average precipitation for the basin stations is 691.8 mm.

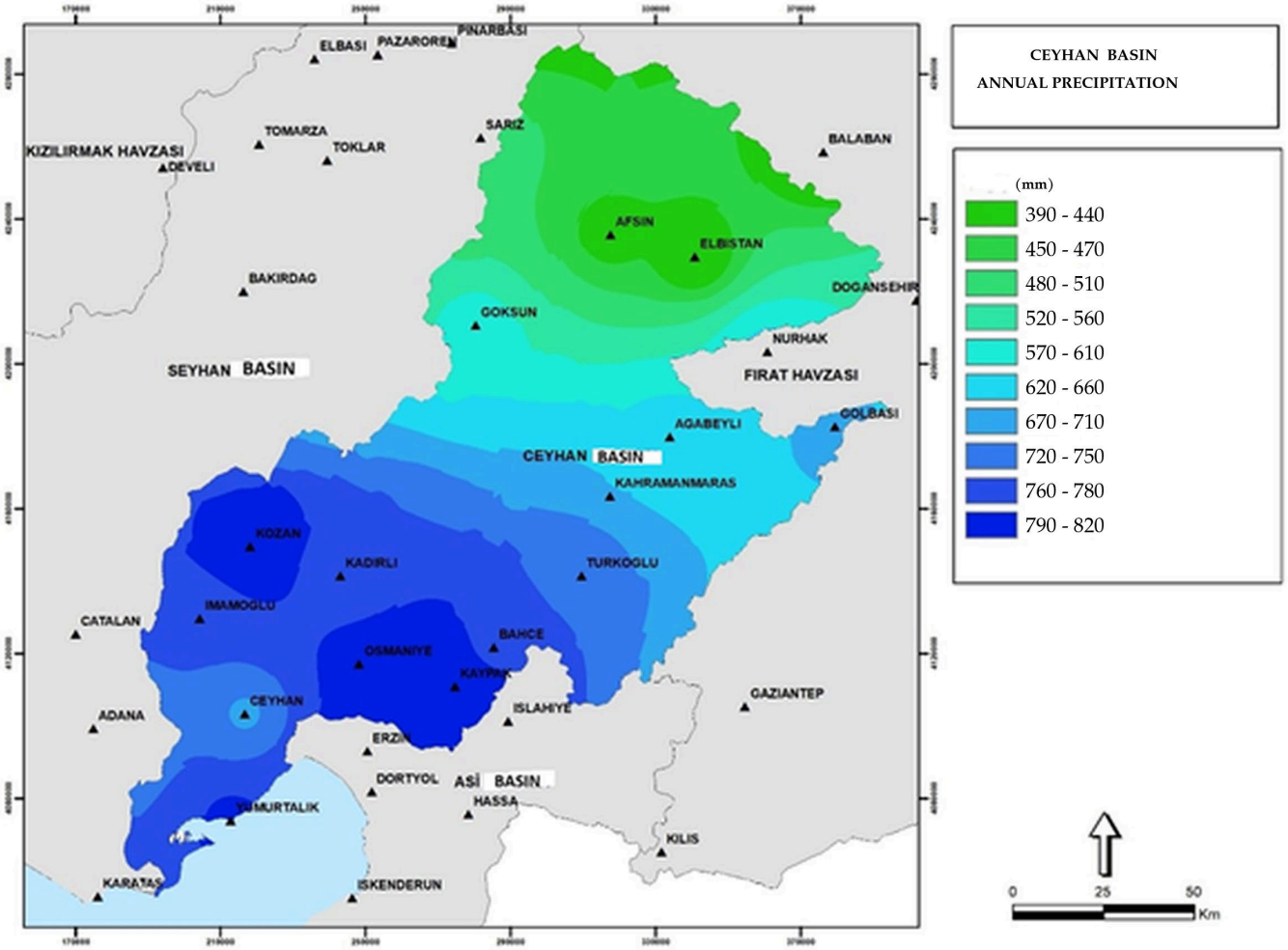


Figure 3. Precipitation distribution map of the Ceyhan Basin.

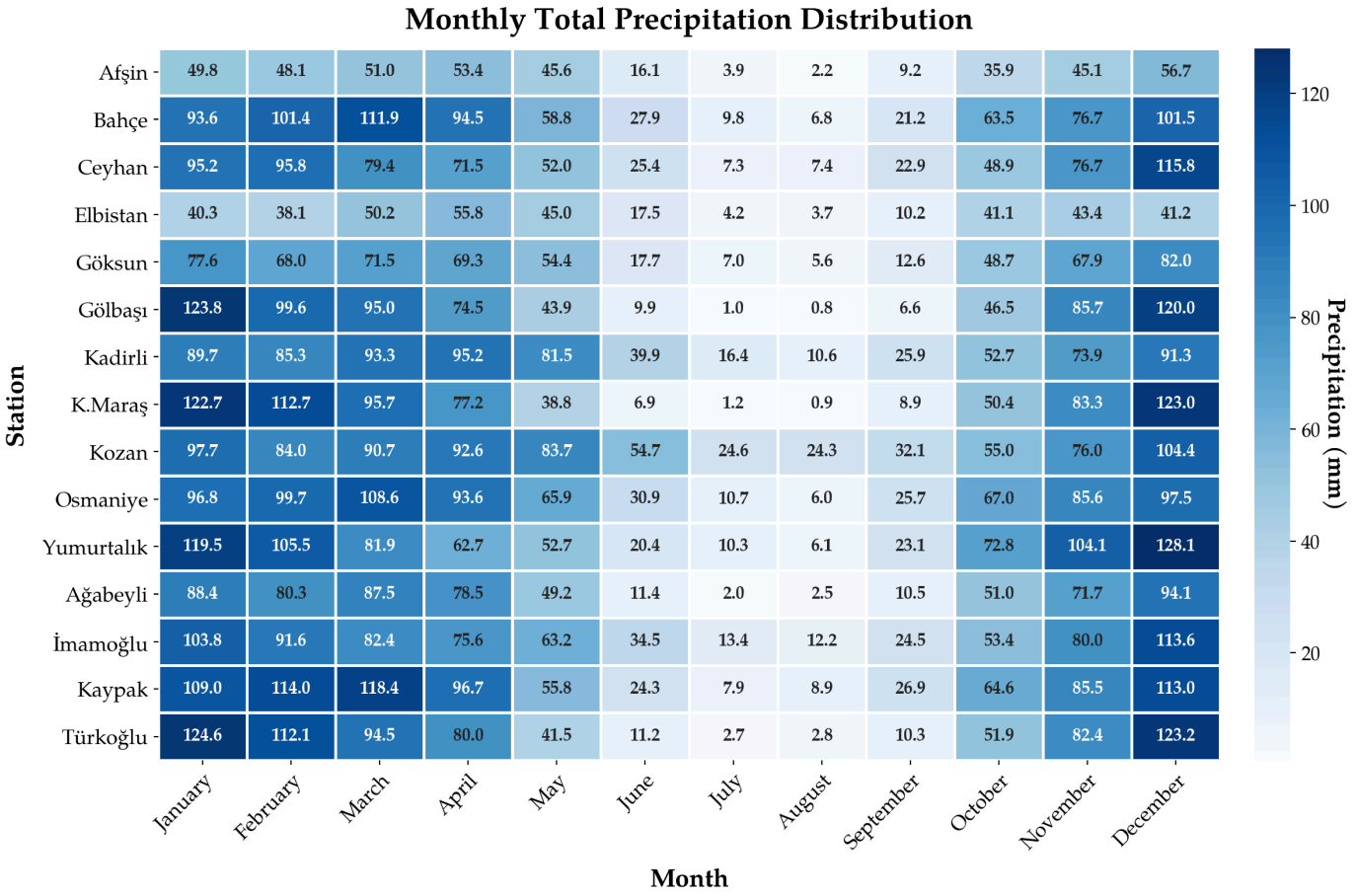


Figure 4. Monthly mean precipitation at meteorological observation stations in the Ceyhan Basin.

The spatial distribution of the annual mean temperature is shown in Figure 5, and a graph of the monthly mean temperatures for the basin stations is given in Figure 6. Like many meteorological variables, temperature is sensitive to altitude and continentality. Stations at sea level record higher temperatures than stations in mountainous areas. Aspect is another important determinant of temperature: stations located on south-facing slopes are warmer than those on north-facing slopes. Looking at the basin's mean monthly temperatures, the highest values occur in July and August (26.4 °C), and the lowest in January (4.6 °C). Kozan station has the highest annual mean temperature (19.4 °C), while Göksun station records the lowest annual mean (8.9 °C). The basin's annual mean temperature is 15.6 °C.

2.2. Methods

2.2.1. Palmer Drought Severity Index (PDSI)

Calculation of the Palmer indices is based on the soil water/moisture balance. The soil water balance generally relies on monthly or weekly total precipitation, monthly or weekly mean air temperature, and the AWHC of the soil for the area under study (a parameter usually treated as fixed). The applicability and reliability of these indices depend on accurate derivation of the input data and parameters (for example, AWHC). Therefore, realistic estimation of soil moisture is crucial in these computations [21].

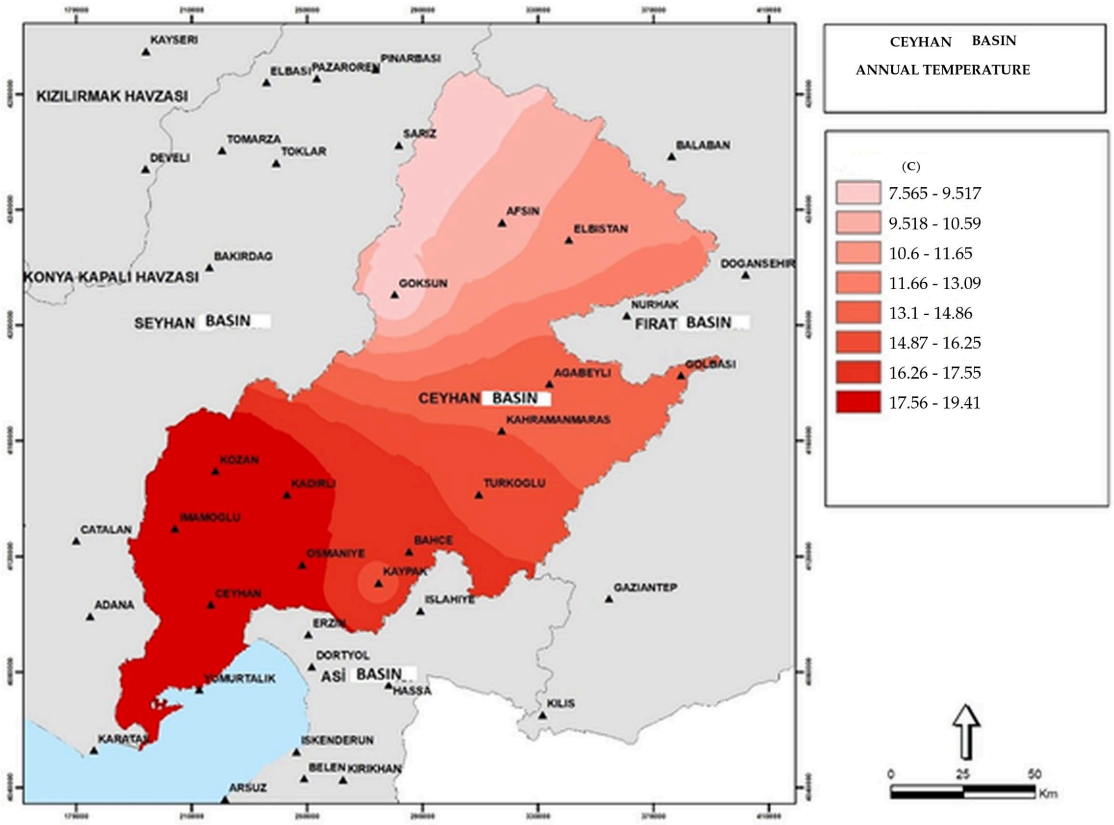


Figure 5. Temperature distribution map of the Ceyhan Basin.

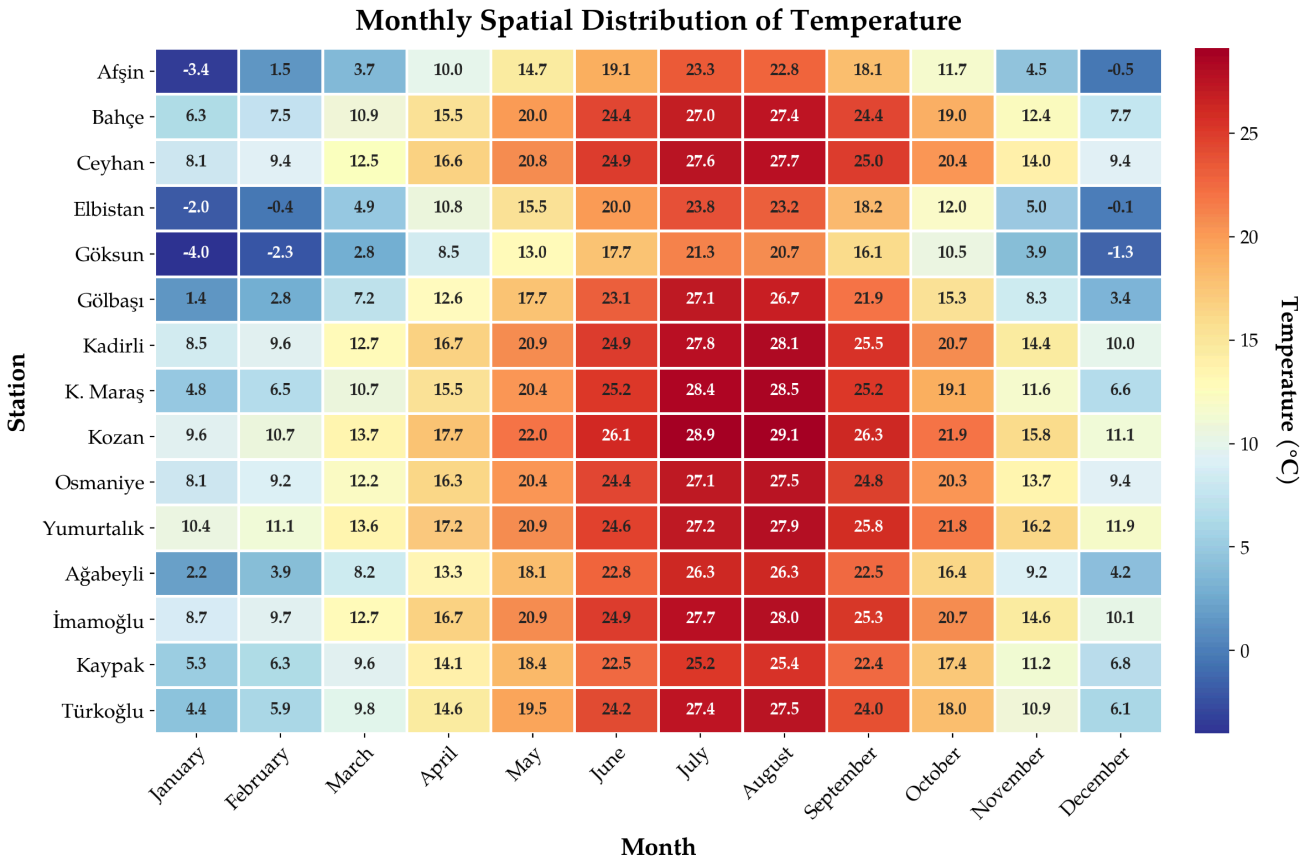


Figure 6. Monthly mean temperatures at meteorological observation stations in the Ceyhan Basin.

The Palmer Drought Severity Index (PDSI), derived by combining temperature and precipitation data with a simple water balance model, was originally developed to identify drought conditions in agricultural regions of the United States [21]. Machine learning and artificial intelligence methods have further improved traditional drought indices such as PDSI, increasing prediction accuracy and model reliability [40,41].

The Palmer Drought Severity Index (PDSI) can be applied even in regions with limited data when sufficient input parameters are available [42]. The Palmer Drought Severity Index (PDSI) has been proposed to improve drought management [43]. The Palmer Drought Severity Index (PDSI) is a widely used regional drought index for monitoring drought events and examining the spatial extent and severity of drought periods [16]. Some researchers have suggested that PDSI is suitable for assessing agricultural drought in the south-central United States [44]. Wu [45] developed a Soil Moisture Deficit Index (SMDI) that measures drought severity using weekly data from his model. This index was found to show a strong correlation with PDSI. To eliminate imbalances and ensure comparability between drought indices, different methods of PDSI have been proposed [46].

PDSI is computed using monthly precipitation, temperature, and soil available water-holding capacity. The Palmer computation procedure is based on the water balance and yields estimates of fundamental water-balance components such as evapotranspiration, water entering the soil, surface runoff, and moisture loss from the surface; anthropogenic influences such as irrigation are not included. PDSI is typically calculated on a monthly basis: positive values indicate moist conditions and negative values indicate dry (drought) conditions. The PDSI may be computed iteratively as [47]:

$$X_i = X_{i-1} + \frac{Z_i}{3} - 0.103 * X_{i-1} \quad (1)$$

where X_i is the PDSI value for month i and Z_i represents the (monthly) moisture departure term used in Palmer's formulation.

To classify the onset and cessation of dry or wet spells, Palmer's general equation is partitioned into three indices that indicate the beginning of wet or dry periods and whether a wet or dry spell has begun:

X_1: intensity index that indicates the start of a wet period (always positive);

X_2: intensity index that indicates the start of a dry period (always negative);

X_3: index that identifies the beginning of any wet or dry period and, because it characterizes ongoing or previously active events, carries broad information about drought severity and is therefore particularly important.

According to Palmer [21], PDSI values of $\geq$+4.00 indicate extremely wet conditions, whereas values of ≤ -4.00 indicate extreme drought conditions. Intermediate positive values represent progressively wetter conditions, ranging from the onset of a wet spell to very wet conditions, while negative values indicate progressively drier conditions, ranging from the onset of a dry spell to severe drought. The commonly used PDSI drought and moisture severity classes and their corresponding threshold values are presented in Table 3, following the classification proposed by Palmer [21] and summarized by Türkeş et al. [47].

Table 3. PDSI drought classification and threshold values.

Threshold Values	Drought/Moisture Class
$\geq$4.00	Extremely Wet
3.00–3.99	Very Wet
2.00–2.99	Moderately Wet
1.00–1.99	Slightly Wet
0.50–0.99	Onset of Wet Spell

Table 3. *Cont.*

Threshold Values	Drought/Moisture Class
0.49–−0.49	Near Normal
−0.50–−0.99	Onset of Dry Spell
−1.00–−1.99	Mild Drought
−2.00–−2.99	Moderate Drought
−3.00–−3.99	Severe Drought
≤−4.00	Extreme Drought

2.2.2. Palmer Hydrological Drought Index (PHDI)

The Palmer Hydrological Drought Index (PHDI), derived from the original PDSI calculations, takes into account the long-term hydrological effects on groundwater, stream flow, and water storage capacity [48]. The index, which needs uninterrupted monthly temperature and precipitation data, allows quantitative comparison of droughts in different times and places thanks to its standardized structure. A distinctive feature of the PHDI is its definition of drought termination; the index considers drought to end only when the moisture deficit is completely eliminated. Accordingly, by comparing the amount of moisture received with the required moisture amount, one can estimate the exact end time of drought events [17]. PHDI is useful because it considers droughts that may impact water resources over long durations. The water balance approach underlying the method enables assessment of the integrated water system. However, some disadvantages of PHDI are:

i. It does not account for runoff generated by snowmelt [49];
ii. It may be insufficiently effective in regions with high variability of precipitation or streamflow [50];
iii. It does not include irrigation systems or other human-induced effects in the computations [13];
iv. Frequency characteristics may vary by region and time (for example, extreme drought may not be a rare event during some months).

The widely used PDSI severity classes and thresholds are also applied to PHDI.

$$X_i = 0.897 * X_(i - 1) + (Z_i)/3 \quad (2)$$

Here:

X_i: PHDI value for the current month (current period)

$X_(i - 1)$: PHDI value from the previous month (persistence coefficient)

Z_i: Palmer Moisture Anomaly Index for the current month (monthly climatic humidity deviation).

2.2.3. Self-Calibrating Palmer Hydrological Drought Index (scPHDI)

Since the empirical coefficients of the traditional PHDI are initially determined mainly according to US conditions, they cannot fully reflect the climate structure of different regions [19]. The Self-Calibrating Palmer Hydrological Drought Index (scPHDI), developed to overcome this limitation, dynamically calculates all coefficients on a station-by-station basis according to the local climate regime. Thanks to this regional adaptation capability, scPHDI has been used as a composite index component for drought monitoring and early warning systems in China [51]; in agricultural analyses in the USA, it was reported as the most successful drought indicator, especially for corn among the basic crops studied [20].

In Palmer drought calculations (PDSI, PHDI, and scPHDI), in addition to temperature and precipitation, the soil's AWHC is required. The water that plants can extract from the soil is termed usable water. Usable water refers to the amount of soil water available

for plant uptake between field capacity (FC) and the permanent wilting point (WP). The AWHC is obtained as the difference between field capacity and wilting point [52]:

$$AWHC = FC - WP \quad (3)$$

The amount of usable water varies with soil texture, organic matter content, and pore characteristics. Usable water data can be obtained from the global SoilGrids datasets produced by ISRIC (International Soil Reference and Information Centre), published in 2014 as 250 m (Soil Grids 250 m) and 1 km (Soil Grids 1 km) spatial resolution soil layers [53]. This dataset contains the most up to date global soil information produced using machine learning and statistical analyses. It provides volumetric percentages of usable water at various depths (0, 5, 15, 30, 60, 100, and 200 cm) and at field capacity tensions (pF = 2.0, pF = 2.3, pF = 2.5).

Within the project, the usable water amount was prepared for Palmer drought analyses using a depth-weighted integration approach for the upper 100 cm soil profile. Specifically, the volumetric percentages of usable water provided for individual SoilGrids depth intervals (e.g., 0–5, 5–15, 15–30, 30–60, and 60–100 cm) were multiplied by their respective layer thicknesses and summed to obtain the total usable water capacity for the entire 100 cm column.

To utilize these spatially continuous grid layers in our station-based drought analyses, the resulting raster values were assigned to specific stations by extracting the pixel values at the exact geographical coordinates of the meteorological stations using spatial point-extraction tools in a GIS environment. Finally, these estimates were validated against field-determined usable water values at selected basin locations. Reference mean air temperature values required for Palmer drought calculations were obtained from the 55-year (1970–2024) records of the meteorological stations. As an intermediate step in obtaining Palmer index values, potential evapotranspiration (PET) and evapotranspiration estimates were computed using the Thornthwaite method [54] for ease of use (it requires only monthly mean temperature data). More accurate PET estimates can be obtained using the Penman Monteith method; however, because Palmer indices are generally not highly sensitive to the PET formulation used during drought periods [55], the Thornthwaite method was adopted in this study.

The comparison between SoilGrids and field-measured AWHC values yielded an R^2 of 0.65, indicating that SoilGrids explained 65% of the observed variability. The RMSE was 22.5 mm, equivalent to approximately 16% of the mean AWHC (140 mm), while the bias was 0 mm, indicating no systematic overestimation or underestimation. Field-measured AWHC ranged from 90 to 190 mm, suggesting substantial spatial variability that SoilGrids partially captured. However, the small validation sample (N = 10) introduces uncertainty into the estimated performance metrics; therefore, these results should be interpreted with caution. The sensitivity analysis examined the effects of AWHC uncertainty on drought classification. Under both ±20% and ±50% perturbations, the drought-index series remained strongly correlated with the baseline, and the main historical drought events (1989, 2007–2008, and 2017) were consistently identified. These correlations indicate agreement between perturbed and baseline series rather than independent validation of SoilGrids. Changes in drought classification and severe drought frequency were relatively limited under the ±20% scenario, whereas the ±50% scenario produced larger, although still moderate, changes (Table 4). These results indicate that the principal drought patterns are relatively robust to plausible uncertainty in AWHC, while the effects of larger AWHC perturbations become more evident in individual months and drought-frequency estimates.

Table 4. Sensitivity of drought classification to AWHC.

AWHC Scenario	Drought Index	Correlation with Baseline (r)	Months with Changed Classification (%)	Change in Severe Drought Frequency (Percentage Points)	Key Events Retained (1989, 2007–08, 2017)
±20%	PDSI/PHDI	>0.97	5–10	±1–2	Yes
±20%	scPHDI	>0.98	3–6	±0.5–1.5	Yes
±50%	PDSI/PHDI	>0.90	12–25	±3–5	Yes
±50%	scPHDI	>0.93	8–15	±2–3	Yes

The Palmer drought index calculation code has long been operational and widely available to researchers. Although many drought indices have been developed, Palmer analyses continue to be widely used worldwide. The main advantages of these indices are that they incorporate soil information into the water budget calculation, they have abundant applications in academic literature, and the computation code is openly available [13]. Constraints on the index's use [15,22] include the requirement for complete time-series input data, the time lag introduced in drought detection due to simplification of soil-moisture dynamics, suboptimal performance under frozen precipitation and frozen ground conditions, and original calibration primarily for the United States.

2.2.4. Standardized Runoff Index (SRI12) and Validation Datasets

To provide physical evidence of hydrological drought that is less directly constrained by the reconstructed meteorological forcing, the Standardized Runoff Index at a 12-month timescale (SRI12) was calculated using monthly streamflow records [36]. Monthly discharge data (m^3/s) covering the period 1970–2024 were obtained from key Stream Gauging Stations (AGI) operated by the State Hydraulic Works (DSİ) and the General Directorate of Water Management, including stations E20A001, E20A004, and E20A005 located along the Ceyhan River and its major tributaries. Missing monthly streamflow records were reconstructed using non-linear hydrometric regression models developed from strongly correlated adjacent stations within the same sub-basin network ($r > 0.88$) [56]. For short and isolated gaps of fewer than three consecutive months, monthly mean proportion imputation was applied based on long-term seasonal runoff patterns. Because the reconstructed months depend on the same regional hydroclimatic signal, the reconstructed part of the SRI12 series is not fully independent of the meteorological forcing, and SRI12 is therefore regarded as partly rather than fully independent evidence. To ensure strict temporal consistency with the 12-month meteorological indices (SPI12 and SPEI12) and the long-memory Palmer indices (PHDI and scPHDI), SRI12 was calculated using a 12-month moving accumulation window ending in month m of year y. This approach accounts for the seasonal accumulation of river runoff and the catchment-scale response time to cumulative precipitation and soil-moisture deficits. In addition to SRI12, non-meteorological corroborating evidence was obtained from official agricultural statistics, including cultivated area and yield records for wheat and cotton in the Ceyhan district for 2002–2015, together with localized groundwater extraction indicators, including pumping depth and energy consumption records provided by the Ministry of Agriculture and Forestry. These datasets were used to assess the consistency between hydrological drought signals and their corresponding agricultural and groundwater impacts. Because consistent district-level statistics were available only for 2002–2015, the agricultural interpretation in this study is confined to this period and is not extrapolated to the full 1970–2024 drought record. SPI12 and SRI12 were standardized with gamma distributions fitted separately for each calendar month over the full 1970–2024 record (SPEI12: three-parameter log-logistic), and a fixed 1971–2000 baseline was tested in a sensitivity analysis (Supplementary Table S1).

3. Results

Time-series of Palmer drought indices for the Ceyhan Basin were computed. Monthly values of the Palmer Drought Severity Index (PDSI), the Palmer Hydrological Drought Index (PHDI), and the self-calibrating PHDI (scPHDI) were first calculated for each station in the basin and then spatially aggregated to represent the entire Ceyhan Basin using weighted averages. Table 5 shows that all drought indices for the period 1970–2024 indicate a significant increase in drought conditions, particularly from the late 1980s and the 2000s onwards.

Table 5. Comparative assessment of temporal drought characteristics based on PDSI, PHDI, and scPHDI during 1970–2024, including general trends, identified drought periods, severe drought events, and overall drought evolution.

Index	Period	General Trend	Drought Periods (Negative Values)	Severe Drought ($\approx \leq -3$)
PDSI	1970–2024	Alternating wet and dry periods are observed throughout the record.	Pronounced drought periods occurred during 1970–1975, 1987–1990, 2001–2009, and 2014–2024.	Severe droughts occurred around 1989, 2007–2008, and 2017.
PHDI	1970–2024	Shows temporal fluctuations similar to PDSI.	Negative anomalies are evident during 1970–1975, 1988–1990, 1999–2001, 2005–2009, and 2015–2024	Strong drought signals were detected in 1989, 2007–2008, and 2017.
scPHDI	1970–2024	Displays frequent transitions between wet and dry conditions and considerable temporal variability.	Negative trends dominated during the 1970s, 1988–1990, 2000–2002, 2005–2009, and 2014–2024	Severe drought conditions occurred during 1989 and 2007–2008.

The variation in SC-PHDI values across stations reveals that drought conditions show significant spatial differences. The lowest SC-PHDI values were observed at Elbistan and İmamoğlu stations at levels below 5% or lower. High values are noteworthy at Kadirli and Kozan stations, while moderate variations are observed at Ceyhan, Göksun, and Kahramanmaraş stations (Figure 7. In general, these differences in SC-PHDI values demonstrate the influence of climatic variability, topographic features, and hydroclimatic conditions on drought severity within the basin. These results indicate that drought effects are not homogeneous in the Ceyhan Basin and that there are different drought dynamics at the station level.

Averaging across stations within the basin yields basin-level occurrence rates of severe drought = 10.8%, moderate drought = 15.1%, and mild drought = 18.2%. The distributions of the Palmer and standardized indices for the basin are compared in Figure 8. Basin-wide drought severity and occurrence rates clearly indicate the presence of drought, particularly after 2002. Considering station-based evaluations for the Ceyhan district as an example: annual precipitation is lower than in neighboring districts (approximately 570–610 mm), while mean annual temperature is about one degree higher (approximately 17.56–19.41 °C). According to data from the Ministry of Agriculture, Forestry, and Water Affairs for 2002–2015, both the cultivated area and the total production of the region's two most important crops declined sharply, whereas their unit yields increased (Table 5).

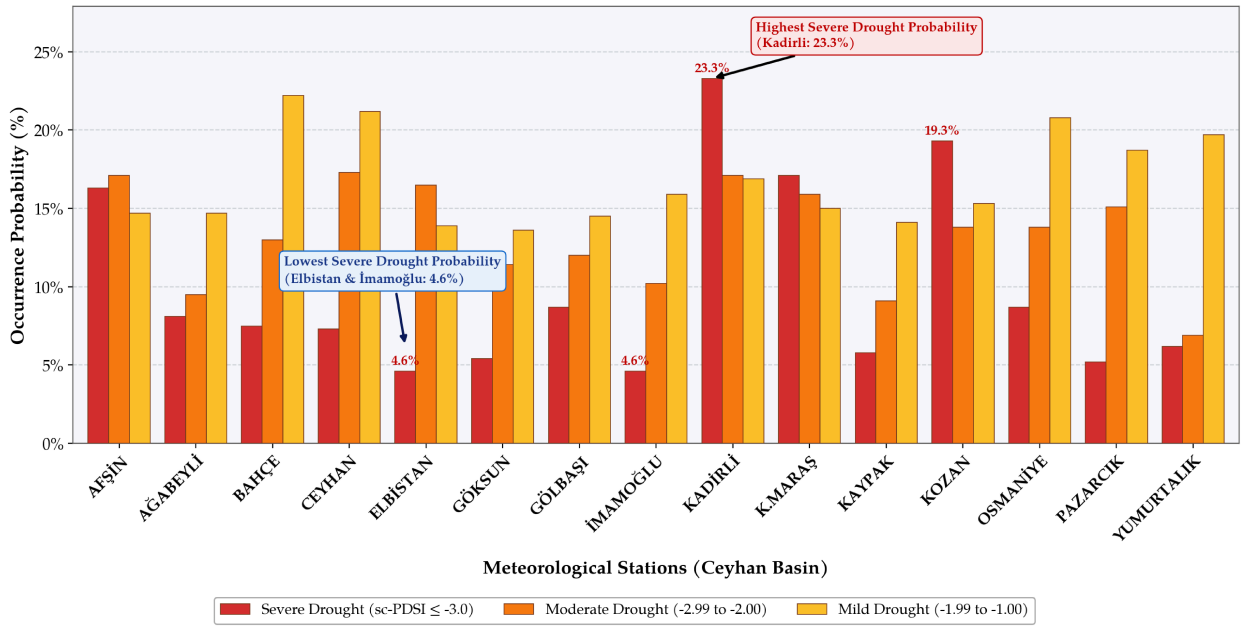


Figure 7. Probability of scPHDI drought occurrence for stations within the Ceyhan Basin.

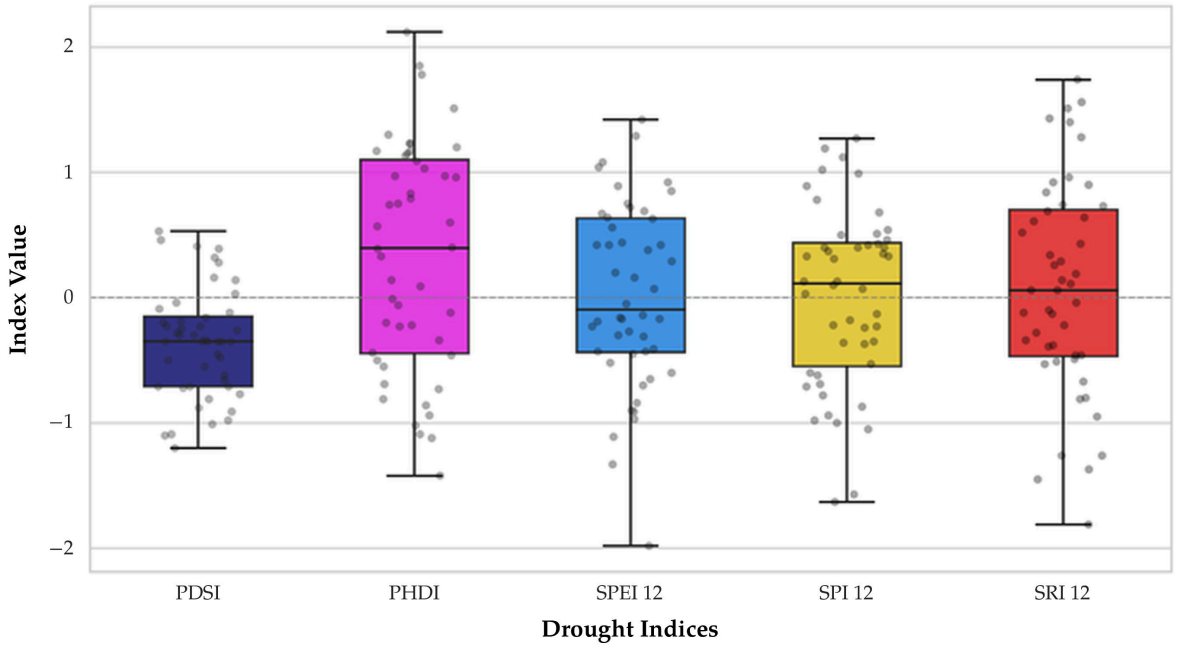


Figure 8. Comparison of PDSI, PHDI, SPEI12, SPI12, and SRI12 for the Ceyhan Basin.

An examination of agricultural statistics for the Ceyhan district between 2002 and 2015 indicates complex dynamics in crop production (Table 6). While total production of wheat and cotton declined significantly, this was predominantly driven by a major contraction in cultivated area rather than a decline in productivity per unit land. In fact, crop yields per unit area increased from 0.381 to 0.448 t/da (+17.6%) for wheat and from 0.283 to 0.532 t/da (+88.1%) for cotton over the same period. The increase in unit yield suggests that agricultural management practices, technological enhancements, and optimized inputs have improved crop efficiency. Conversely, the reduction in total cultivated area reflects broader land use shifts influenced by multiple interacting drivers, including water availability, increasing pumping costs due to deeper groundwater tables, crop switching, market price fluctuations, and regional agricultural support policies. The

slowly progressing agricultural drought in the basin, particularly given its location in the Mediterranean region, which is expected to be among the most affected by climate change, indicates that more dramatic consequences may arise in the future. These agricultural interpretations are confined to the 2002–2015 data window and are not extrapolated to the full 1970–2024 drought record. The flow trend of the Ceyhan River passing through the Ceyhan District within the basin, presented in Figure 8 also supports this assessment [30].

Table 6. Agricultural cultivated area, total production, and unit yield in the Ceyhan District.

Crop	Cultivated Area (da) (2002)	Production Amount (tons) (2002)	Yield (t/da) (2002)	Cultivated Area (da) (2015)	Production Amount (tons) (2015)	Yield (t/da) (2015)	Yield Change (%)
Wheat	746,600	284,252	0.381	256,658	114,927	0.448	+17.6%
Cotton	125,020	35,359	0.283	36,450	19,391	0.532	+88.1%

Figure 9 shows a predominantly decreasing trend in annual streamflow at the Ceyhan River stations. Significant negative trends were detected at E20A001 ($Z = -2.341$; $p = 0.019$) and E20A005 ($Z = -3.085$; $p = 0.002$), with Sen's slope estimates of -1.125 and -1.840 m^3/s/year, respectively. In contrast, E20A004 showed no statistically significant trend ($p = 0.970$). These results indicate spatially heterogeneous but generally declining streamflow conditions across the analyzed stations.

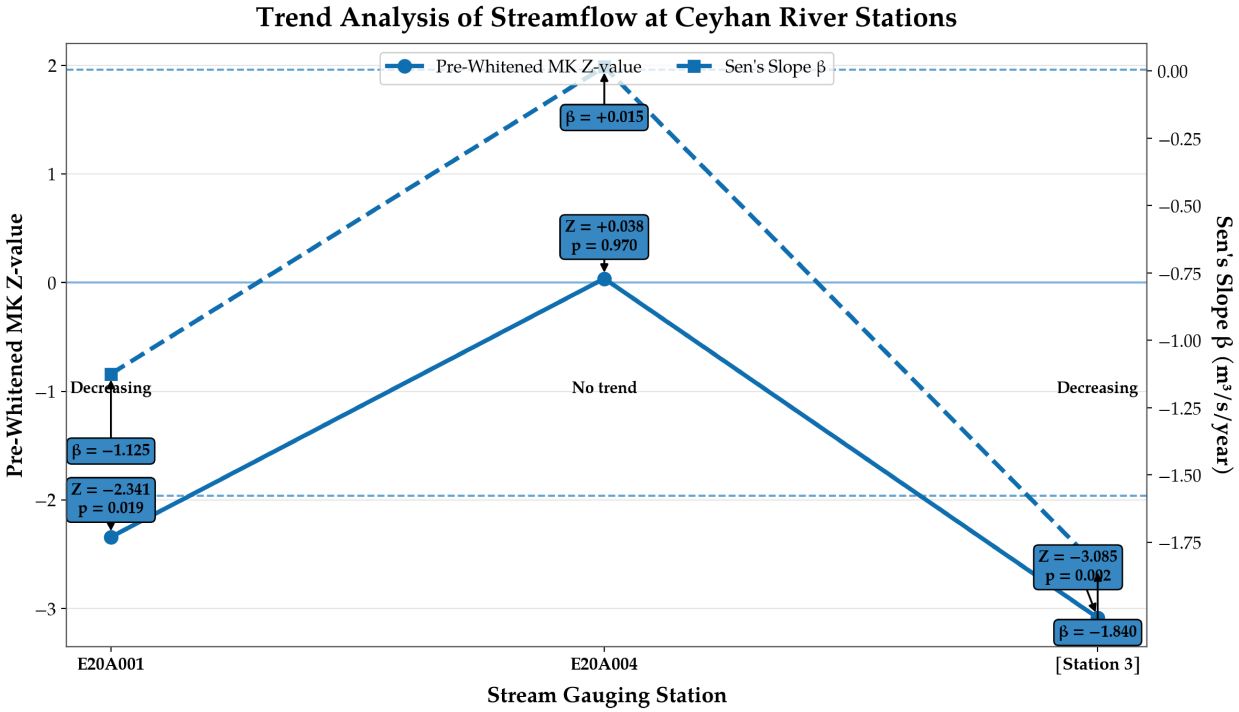


Figure 9. Statistical trend analysis of annual natural streamflow at selected stations in the Ceyhan Basin (1970–2024), showing Lag-1 autocorrelation, pre-whitened Mann–Kendall Z-values, *p*-values, Sen's slope magnitudes, and corresponding trend directions.

The results indicate significant decreasing trends at stations E20A001 and E20A005, with Sen's slopes of -1.125 and -1.840 m^3/s/year, respectively. Their 95% confidence intervals remain entirely below zero, supporting the statistical significance of the detected decreases. In contrast, E20A004 shows no significant trend ($p = 0.970$), and its confidence interval spans zero (Table 7). Overall, the results suggest spatial heterogeneity in streamflow trends, with stronger declines at E20A005 than at E20A001 (Figure 10).

Table 7. Trend results with Sen's slope and 95% confidence intervals.

Station	Z	*p*-Value	Sen's Slope (m^3/s/Year)	95% CI (m^3/s/Year)	Relative Slope (%/Decade)	Trend
E20A001	−2.341	0.019	−1.125	−2.1 to −0.2	≈−10	Significant decreasing
E20A004	+0.038	0.970	+0.015	−0.9 to +0.9	≈+0.1	No significant trend
E20A005	−3.085	0.002	−1.840	−3.0 to −0.7	≈−13	Significant decreasing

The supplementary analyses indicate that precipitation and streamflow reconstructions provide generally consistent performance across stations and seasons. Drought-event characteristics remain broadly stable under alternative AWHC assumptions, while incorporating a degree-day snow module produces only limited changes in drought classification and timing. Overall, these sensitivity analyses support the robustness of the reconstructed drought signals (Supplementary Table S2).

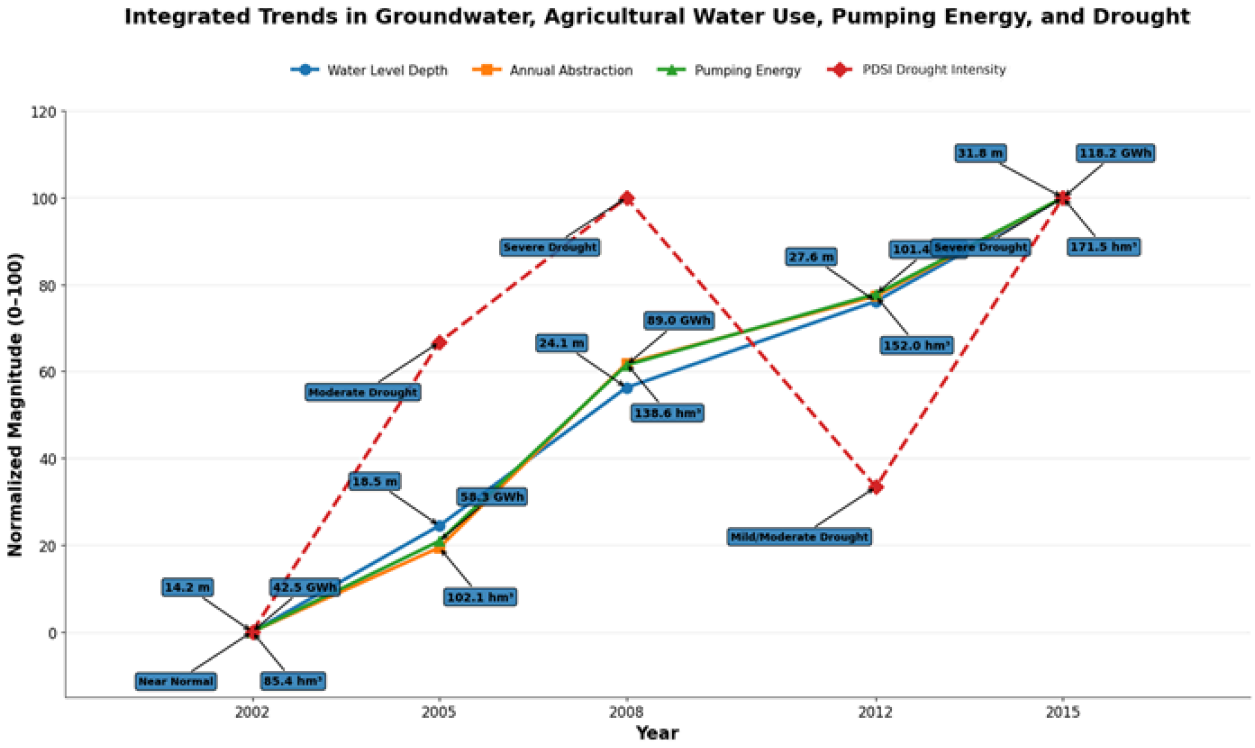


Figure 10. Integrated temporal trends in mean static water level depth, annual groundwater abstraction, agricultural pumping energy consumption, and PDSI drought intensity during 2002–2015. Values are presented on a normalized scale (0–100) to facilitate comparison among variables with different units. Arrows indicate the corresponding observed values and drought-state classifications for each year.

4. Discussion

The results of this study demonstrate that the Palmer family of indices (PDSI, PHDI, and scPHDI) provides a coherent and consistent picture of agricultural and hydrological drought conditions in the Ceyhan Basin over the 1970–2024 period. The clustering of severe and moderate drought episodes after 2002, evident in both the basin-wide index series (Table 4) and the station-based occurrence probabilities (Figures 7 and 8), indicates a discernible shift in the basin's drought regime rather than an isolated short-term anomaly. This is consistent with the broader literature identifying the Mediterranean region as one of the areas most vulnerable to climate-change-driven aridification [57–59].

The station-level results also reveal considerable spatial heterogeneity within a relatively compact basin. Stations such as Kadirli consistently showed the highest severe drought occurrence rates under both PDSI and scPHDI, whereas İmamoğlu and Elbistan showed the lowest. This spatial contrast is unlikely to be explained by precipitation totals

alone and more probably reflects differences in local topography, soil water-holding capacity, and the timing of the water balance components used in the Palmer formulation. The generally close correspondence between PDSI and scPHDI patterns supports the expectation that meteorological water deficits propagate into hydrological deficits with some delay, although the modestly higher occurrence rates obtained for scPHDI at several stations suggest that hydrological drought in the basin tends to be somewhat more persistent than its meteorological counterpart, in line with the cumulative, longer-memory design of the PHDI/scPHDI formulation.

The agreement between the Palmer indices and the SPI12, SPEI12, and SRI12 series provides additional corroborating evidence, although its evidential strength varies across the benchmarks. Because SPI12 and SPEI12 are also derived from precipitation-based meteorological forcing, their agreement with the Palmer indices represents consistency among meteorological drought indicators rather than fully independent validation. In contrast, agreement with the streamflow-based SRI12 provides a more independent line of evidence, particularly for months with observed streamflow records, because it reflects hydrological rather than solely meteorological conditions. This interpretation is consistent with recommendations in the drought-monitoring literature [60,61], which emphasize that no single drought index should be interpreted in isolation and that convergence among complementary meteorological and hydrological indicators can provide a more robust basis for drought assessment and operational decision-making.

Independent of the observed streamflow months, only evidence for the detected drought signal is provided by non-meteorological variables. The correspondence between the Palmer hydrological indices (PHDI/scPHDI) and the streamflow-derived SRI12 indicates that the calculated soil-moisture deficits are consistent with surface-water shortages across the basin's drainage network, although streamflow in the Ceyhan Basin is also affected by reservoir regulation and abstraction.

Beyond the hydroclimatic evidence, the study's agricultural and socio-economic indicators point in the same direction. The temporal overlap between the severe post-2002 drought episodes detected by the Palmer indices and the reduction in total cultivated area for wheat and cotton in the Ceyhan district during 2002–2015 (Table 5) provides contextual evidence of changing agricultural conditions. However, unit yield data reveal that productivity per decare actually improved during this period (+17.6% for wheat and +88.1% for cotton), demonstrating that land contraction rather than reduced unit productivity accounted for the drop in overall harvest. Therefore, land allocation decisions cannot be attributed strictly to hydroclimatic deficits alone. Instead, intensifying drought conditions and falling groundwater levels likely amplified operational challenges (such as increased energy costs for groundwater extraction), driving farmers toward alternative crop selection, reduced planting acreage, or land abandonment alongside external economic and policy pressures. The reported increase in groundwater-abstraction depths, and the associated rise in pumping-related energy consumption, is a further symptom of the same pressure: it is consistent with an increasing reliance on groundwater as surface-water and soil-moisture deficits intensify, although abstraction also responds to non-climatic drivers such as crop choice, energy prices, and licensing; such reliance is, in the long run, neither sustainable nor climate-resilient [3,7].

The decreasing trend detected in the natural flows of the Ceyhan River at the upstream stations (E20A001 and E20A005), in contrast to the absence of a significant trend at the downstream station (E20A004) (Figure 10), is a plausible hydrological corollary of the drought signal identified by the Palmer indices. Upstream sub-basins, which are more directly governed by local precipitation and snowmelt inputs and are less buffered by downstream regulation and tributary inflows, would be expected to respond more quickly

and more visibly to a sustained precipitation deficit. This spatial pattern reinforces the case for sub-basin-scale drought assessment rather than relying exclusively on basin-averaged indicators, since local vulnerabilities can otherwise be masked when data are aggregated over the whole basin.

From a practical standpoint, these findings support the view, already noted in existing studies of the Ceyhan Basin, that the priority for the region is not the development of new drought indices but the consistent operational use of established indices—in this case, the self-calibrating Palmer indices for drought monitoring within a drought-management framework [31,62]. Because PDSI and scPHDI recalibrate their duration factors and climatic characteristics to local conditions [25], they are particularly well suited to a basin such as the Ceyhan, whose climatic regime differs from the U.S. Great Plains setting for which the original Palmer index was developed [22,55]. Embedding threshold values derived from the present analysis into a basin drought-management plan, together with targeted agricultural support and groundwater-use regulation, would represent a concrete step toward translating these results into risk-reduction practice. It should be emphasized, however, that the present analysis is retrospective and characterizes monitoring capability only; forecasting skill—warning lead time, probability of detection and false alarms in a hindcast setting—was not evaluated. The indices should therefore be regarded as potentially useful components of an early-warning system whose predictive capability remains to be demonstrated.

To substantiate the physical impact of prolonged agricultural drought on regional hydrogeology, static water level (SWL) observation records from state monitoring wells (GW wells) across the Lower Ceyhan Plain (including the Ceyhan district) were analyzed alongside agricultural groundwater abstraction and electricity usage statistics for agricultural pumping (2002–2015).

As presented in Table 8, the mean static groundwater depth in the Ceyhan district dropped from 14.2 m in 2002 to 31.8 m in 2015, representing an average groundwater table decline rate of −1.35 m/year ($p < 0.01$). Concurrently with the drought episodes captured by the scPHDI indices, licensed and unlicensed groundwater abstractions increased significantly. Consequently, total electricity consumption dedicated to agricultural groundwater pumping in the Ceyhan plain rose from 42.5 GWh in 2002 to 118.2 GWh in 2015 (+178.1%). These changes indicate an association between agricultural drought and increased reliance on deep groundwater reserves and higher energy costs for irrigation; however, because abstraction itself lowers water levels regardless of climate, and temporal precedence was not tested, this concurrence does not by itself demonstrate causality.

Table 8. Groundwater static levels, estimated abstraction volumes, and agricultural pumping energy consumption in Ceyhan District (2002–2015).

Year	Mean Static Water Level Depth (m)	Annual Abstraction Volume (hm^3)	Agricultural Pumping Energy Usage (GWh)	PDSI Anomaly State
2002	14.2	85.4	42.5	Near Normal
2005	18.5	102.1	58.3	Moderate Drought
2008	24.1	138.6	89.0	Severe Drought
2012	27.6	152.0	101.4	Mild/Moderate Drought
2015	31.8	171.5	118.2	Severe Drought

The integrated temporal analysis reveals a clear and systematic intensification of groundwater stress between 2002 and 2015. Mean static water level depth increased from 14.2 m to 31.8 m, indicating a substantial decline in groundwater availability. During the same period, annual groundwater abstraction increased from 85.4 to 171.5 hm^3, while

agricultural pumping energy consumption rose from 42.5 to 118.2 GWh. The concurrent increase in groundwater withdrawal and pumping energy suggests that declining groundwater levels required progressively greater energy inputs to maintain agricultural water supply. This pattern coincided with a shift from near-normal conditions in 2002 toward moderate and severe drought conditions, with severe drought observed in 2008 and 2015 (Figure 10).

Limitations and Uncertainties

Several sources of uncertainty affect the results. First, 5.8% of the monthly precipitation and 2.9% of the monthly temperature values were reconstructed with PRISM. Because the precipitation RMSE of the leave-one-out validation (14.8 mm) is comparable to the monthly totals of the driest months, reconstruction errors may be proportionally larger in the dry season and may propagate into the water balance in the low-precipitation months on which drought onset depends; interpolation errors are also likely to be larger in the mountainous parts of the basin, where the station network is sparser. Second, approximately 12% of the monthly streamflow values were reconstructed by regression or seasonal-proportion imputation. These months inherit the regional hydroclimatic signal and are not fully independent of the meteorological forcing, so SRI12 provides independent evidence only for observed streamflow months. Third, the Palmer indices rely on a single AWHC value per station derived from SoilGrids, and errors in this parameter affect the magnitude and persistence of the simulated soil-moisture deficits. Fourth, the Palmer water balance does not represent snow accumulation and melt, irrigation, or reservoir operation, all of which are relevant in the Ceyhan Basin. Fifth, four of the fifteen stations are now closed, so the share of reconstructed values increases towards the end of the record. Sixth, streamflow trends were tested at only three gauging stations (E20A001, E20A004, and E20A005), which limits their spatial generality; the absence of a significant trend at E20A004 could reflect tributary inflows or upstream regulation rather than a weaker drought response. Therefore, the contrast with the upstream stations (E20A001, E20A005) is interpreted as consistent with, but not proof of, a stronger upstream drought response, and its attribution requires additional gauges and reservoir release records. Finally, the agricultural and groundwater records cover only 2002–2015, so they support association rather than causal attribution.

5. Conclusions

This study evaluated the performance of the PHDI and its self-calibrating version (scPHDI) for hydrological drought assessment in the Ceyhan Basin, Türkiye, using long-term hydroclimatic records for 1970–2024. The findings illustrate how Palmer-based hydrological indices can be used to examine drought evolution, persistence, and spatial variability, providing a basis for retrospective drought monitoring at the basin scale.

The results indicate an increase in drought occurrence after the early 2000s, accompanied by more frequent and persistent moderate-to-severe drought episodes. Station-level analyses revealed substantial spatial differences, with severe drought occurrence ranging from 4.6% at Elbistan and İmamoğlu to 23.3% at Kadirli. This variation did not follow a simple inland–coastal or elevation gradient, highlighting the spatial complexity of drought conditions across the basin. The self-calibrating index also indicated persistent drought occurrence during parts of the study period, although the extent to which this pattern reflects long-term changes depends on the index formulation and the characteristics of the observational record.

The comparison with agricultural statistics showed that drought conditions after 2002 coincided with reductions in the total cultivated area of major crops in Ceyhan District during 2002–2015. Meanwhile, yields per decare increased by 17.6% for wheat and 88.1%

for cotton. These contrasting trends suggest that changes in cultivated area and crop productivity should be considered together when interpreting agricultural responses to drought. However, the available data do not establish drought as the sole cause of changes in cultivated area or total production; technological developments, agricultural inputs, irrigation costs, crop selection, and market conditions may also have contributed. Accordingly, basin-level drought management would benefit from considering hydroclimatic indicators alongside agricultural and socioeconomic information.

From a practical perspective, the findings suggest that scPHDI may be useful for retrospective hydrological drought monitoring and could complement other indicators in basin-scale water management. Its suitability for operational early-warning applications, however, remains to be established through predictive evaluation, including warning lead time, probability of detection, and false alarm ratio within a hindcast framework.

Future research could strengthen this assessment by integrating Palmer-based indices with remote sensing products, soil moisture observations, climate model projections, and machine learning approaches. Evaluating predictive performance under different hydroclimatic conditions and extending the analysis to sub-basins and local administrative units would also help clarify spatial differences in drought risk and support the development of more targeted water management and drought adaptation strategies.

Supplementary Materials: The following supporting information can be downloaded at: https://www.mdpi.com/article/10.3390/su182110810/s1. Table S1: Gamma distribution parameters for the 12-month indices (12-month window ending in December). Table S2: Supplementary validation, reconstruction performance, station characteristics, drought-event statistics, and sensitivity analyses, including (a) leave-one-out reconstruction errors for monthly precipitation by season, station elevation, and dry months; (b) cold-season precipitation and snow fraction at meteorological stations; (c) SoilGrids available water-holding capacity (AWHC) validation and station AWHC range; and (d) streamflow reconstruction, drought-event statistics, sensitivity analyses, and the effect of adding a degree-day snow module on PHDI/scPHDI.

Author Contributions: Conceptualization, M.D., K.Ş., Y.P. and M.A.Ç.; methodology, M.D. and M.A.Ç.; software, Y.P. and M.A.Ç.; validation, M.D., K.Ş., Y.P. and M.A.Ç.; formal analysis, M.D. and M.A.Ç.; investigation, M.D., K.Ş. and Y.P.; resources, M.D. and K.Ş.; data curation, Y.P.; writing—original draft preparation, M.D. and M.A.Ç.; writing—review and editing, K.Ş., Y.P. and M.A.Ç.; visualization, Y.P. and M.A.Ç.; supervision, M.A.Ç.; project administration, M.D.; funding acquisition, M.D. All authors have read and agreed to the published version of the manuscript.

Funding: This research received no external funding.

Data Availability Statement: The data are not publicly available due to data access restrictions and/or institutional confidentiality requirements. The datasets used in this study can be obtained from the corresponding author upon reasonable request, subject to the relevant permissions and data-use restrictions.

Acknowledgments: The author gratefully acknowledges the Ministry of Agriculture, Forestry and Water Affairs, General Directorate of Water Management, for providing the data used in this study. The authors also acknowledge ChatGPT (GPT-4, free version) and Claude for their assistance with language editing and improving the clarity and readability of the manuscript. The authors remain fully responsible for the content, interpretation, and scientific integrity of the work.

Conflicts of Interest: The authors declare no conflicts of interest.

References

1. Srivastav, A.L.; Dhyani, R.; Ranjan, M.; Madhav, S.; Sillanpää, M. Climate-Resilient Strategies for Sustainable Management of Water Resources and Agriculture. *Environ. Sci. Pollut. Res.* **2021**, *28*, 41576–41595. [CrossRef] [PubMed]

2. Tsakiris, G.P.; Loucks, D.P. Adaptive Water Resources Management Under Climate Change: An Introduction. *Water Resour. Manag.* **2023**, *37*, 2221–2233. [CrossRef]
3. Wilhite, D.A.; Sivakumar, M.V.K.; Pulwarty, R. Managing Drought Risk in a Changing Climate: The Role of National Drought Policy. *Weather Clim. Extrem.* **2014**, *3*, 4–13. [CrossRef]
4. Lindner, A.; Stamm, J. Integrating Climate Change Adaptation and Water Resource Management: A Critical Overview. *Standards* **2025**, *5*, 4. [CrossRef]
5. Şekerci, K.; Tuna, M.C.; Doğan, M.Ş. Effects of Reducing Long-Term Groundwater Overdraft in Uluova Micro-Basin. *Appl. Water Sci.* **2025**, *15*, 218. [CrossRef]
6. Şekerci, K.; Tuna, M.C.; Doğan, M.Ş. Integrated Water Operations under Climate Change: Uluova Micro Basin Example. *J. Water Clim. Change* **2024**, *15*, 3689–3701. [CrossRef]
7. Wada, Y.; van Beek, L.P.H.; van Kempen, C.M.; Reckman, J.W.T.M.; Vasak, S.; Bierkens, M.F.P. Global Depletion of Groundwater Resources. *Geophys. Res. Lett.* **2010**, *37*, L20402. [CrossRef]
8. Wilhite, D.A. *Droughts: A Global Assessment*; Hazards and Disasters Series; Routledge: London, UK, 2000.
9. UNDP. *Drought Risk Management*; United Nations Development Programme: New York, NY, USA, 2016.
10. Wilhite, D.A. Integrated Drought Management: Moving from Managing Disasters to Managing Risk in the Mediterranean Region. *Euro-Mediterr. J. Environ. Integr.* **2019**, *4*, 42. [CrossRef]
11. Estrela, T.; Vargas, E. Drought Management Plans in the European Union. The Case of Spain. *Water Resour. Manag.* **2012**, *26*, 1537–1553. [CrossRef]
12. Global Water Partnership Central and Eastern Europe (GWP CEE). *Guidelines for the Preparation of Drought Management Plans: Development and Implementation in the Context of the EU Water Framework Directive*; GWP CEE: Bratislava, Slovakia, 2015. Available online: https://climate-adapt.eea.europa.eu/en/metadata/guidances/guidelines-for-preparation-of-the-drought-management-plans-1/guidelines-preparation-drought/@@download/file/Guidelines%20for%20preparation%20of%20the%20drought%20management%20plans.pdf (accessed on 20 October 2026).
13. Svoboda, M.; Fuchs, B.A. (Eds.) *Handbook of Drought Indicators and Indices*; Integrated Drought Management Programme (IDMP), Integrated Drought Management Tools and Guidelines Series 2; World Meteorological Organization: Geneva, Switzerland, 2017. [CrossRef]
14. Gevaert, A.I.; Veldkamp, T.I.E.; Ward, P.J. The Effect of Climate Type on Timescales of Drought Propagation in an Ensemble of Global Hydrological Models. *Hydrol. Earth Syst. Sci.* **2018**, *22*, 4649–4665. [CrossRef]
15. Zargar, A.; Sadiq, R.; Naser, B.; Khan, F.I. A Review of Drought Indices. *Environ. Rev.* **2011**, *19*, 333–349. [CrossRef]
16. Mishra, A.K.; Singh, V.P. A Review of Drought Concepts. *J. Hydrol.* **2010**, *391*, 202–216. [CrossRef]
17. Keyantash, J.; Dracup, J.A. The Quantification of Drought: An Evaluation of Drought Indices. *Bull. Am. Meteorol. Soc.* **2002**, *83*, 1167–1180. [CrossRef]
18. Heim, R.R. A Review of Twentieth-Century Drought Indices Used in the United States. *Bull. Am. Meteorol. Soc.* **2002**, *83*, 1149–1165. [CrossRef]
19. Vicente-Serrano, S.M.; Beguería, S.; Lorenzo-Lacruz, J.; Camarero, J.J.; López-Moreno, J.I.; Azorin-Molina, C.; Revuelto, J.; Morán-Tejeda, E.; Sanchez-Lorenzo, A. Performance of Drought Indices for Ecological, Agricultural, and Hydrological Applications. *Earth Interact.* **2012**, *16*, 1–27. [CrossRef]
20. Peña-Gallardo, M.; Vicente-Serrano, S.M.; Dominguez-Castro, F.; Quiring, S.; Svoboda, M.; Beguería, S.; Hannaford, J. Effectiveness of Drought Indices in Identifying Impacts on Major Crops across the USA. *Clim. Res.* **2018**, *75*, 221–240. [CrossRef]
21. Palmer, W.C. *Meteorological Drought*; Research Paper No. 45; U.S. Weather Bureau: Washington, DC, USA, 1965.
22. Alley, W.M. The Palmer Drought Severity Index: Limitations and Assumptions. *J. Clim. Appl. Meteorol.* **1984**, *23*, 1100–1109. [CrossRef]
23. McKee, T.B.; Doesken, N.J.; Kleist, J. The Relationship of Drought Frequency and Duration to Time Scales. In *Proceedings of the 8th Conference on Applied Climatology, Anaheim, CA, USA, 17–22 January 1993*; American Meteorological Society: Boston, MA, USA, 1993; pp. 179–184.
24. Dai, A. Characteristics and Trends in Various Forms of the Palmer Drought Severity Index during 1900–2008. *J. Geophys. Res. Atmos.* **2011**, *116*, D12115. [CrossRef]
25. Wells, N.; Goddard, S.; Hayes, M.J. A Self-Calibrating Palmer Drought Severity Index. *J. Clim.* **2004**, *17*, 2335–2351. [CrossRef]
26. van der Schrier, G.; Barichivich, J.; Briffa, K.R.; Jones, P.D. A scPDSI-Based Global Data Set of Dry and Wet Spells for 1901–2009. *J. Geophys. Res. Atmos.* **2013**, *118*, 4025–4048. [CrossRef]
27. Dikici, M.; Aksel, M. Comparison of SPI, SPEI and SRI Drought Indices for Seyhan Basin. *Int. J. Electron. Mech. Mechatron. Eng.* **2019**, *9*, 1751–1762.
28. Dikici, M. Drought Analysis with Different Indices for the Asi Basin (Turkey). *Sci. Rep.* **2020**, *10*, 20739. [CrossRef] [PubMed]
29. Dikici, M. Drought Analysis for the Seyhan Basin with Vegetation Indices and Comparison with Meteorological Different Indices. *Sustainability* **2022**, *14*, 4464. [CrossRef]

30. Dikici, M.; Aksel, M. Comparison of Drought Indices in the Case of the Ceyhan Basin. *Int. J. Environ. Geoinform.* **2021**, *8*, 113–125. [CrossRef]
31. Yuce, M.I.; Esit, M. Drought Monitoring in Ceyhan Basin, Turkey. *J. Appl. Water Eng. Res.* **2021**, *9*, 293–314. [CrossRef]
32. Van Loon, A.F. Hydrological Drought Explained. *WIREs Water* **2015**, *2*, 359–392. [CrossRef]
33. Li, C.; Gu, Y.; Xu, H.; Huang, J.; Liu, B.; Chun, K.P.; Octavianti, T. Spatial Heterogeneity in the Response of Winter Wheat Yield to Meteorological Dryness/Wetness Variations in Henan Province, China. *Agronomy* **2024**, *14*, 817. [CrossRef]
34. Chen, X.; Du, Y.; Han, D. A Multimodal Data-Driven Framework for Enhanced Wheat Carbon Flux Monitoring. *Agronomy* **2025**, *15*, 920. [CrossRef]
35. Vicente-Serrano, S.M.; Beguería, S.; López-Moreno, J.I. A Multiscalar Drought Index Sensitive to Global Warming: The Standardized Precipitation Evapotranspiration Index. *J. Clim.* **2010**, *23*, 1696–1718. [CrossRef]
36. Shukla, S.; Wood, A.W. Use of a Standardized Runoff Index for Characterizing Hydrologic Drought. *Geophys. Res. Lett.* **2008**, *35*, L02405. [CrossRef]
37. Beck, C.; Philipp, A.; Jacobeit, J. Interannual Drought Index Variations in Central Europe Related to the Large-Scale Atmospheric Circulation—Application and Evaluation of Statistical Downscaling Approaches Based on Circulation Type Classifications. *Theor. Appl. Climatol.* **2014**, *121*, 713–732. [CrossRef]
38. Daly, C.; Halbleib, M.; Smith, J.I.; Gibson, W.P.; Doggett, M.K.; Taylor, G.H.; Curtis, J.; Pasteris, P.P. Physiographically Sensitive Mapping of Climatological Temperature and Precipitation across the Conterminous United States. *Int. J. Climatol.* **2008**, *28*, 2031–2064. [CrossRef]
39. Daly, C.; Gibson, W.; Taylor, G.; Johnson, G.; Pasteris, P. A Knowledge-Based Approach to the Statistical Mapping of Climate. *Clim. Res.* **2002**, *22*, 99–113. [CrossRef]
40. Marusov, A.; Grabar, V.; Maximov, Y.; Sotiriadi, N.; Bulkin, A.; Zaytsev, A. Long-Term Drought Prediction Using Deep Neural Networks Based on Geospatial Weather Data. *Environ. Model. Softw.* **2024**, *179*, 106127. [CrossRef]
41. Melese, T.; Assefa, G.; Terefe, B.; Belay, T.; Bayable, G.; Senamew, A. Machine Learning-Based Drought Prediction Using Palmer Drought Severity Index and TerraClimate Data in Ethiopia. *PLoS ONE* **2025**, *20*, e0326174. [CrossRef] [PubMed]
42. Yang, Y.; McVicar, T.R.; Donohue, R.J.; Zhang, Y.; Roderick, M.L.; Chiew, F.H.; Zhang, L.; Zhang, J. Lags in Hydrologic Recovery Following an Extreme Drought: Assessing the Roles of Climate and Catchment Characteristics. *Water Resour. Res.* **2017**, *53*, 4821–4837. [CrossRef]
43. Yu, H.; Zhang, Q.; Xu, C.-Y.; Du, J.; Sun, P.; Hu, P. Modified Palmer Drought Severity Index: Model Improvement and Application. *Environ. Int.* **2019**, *130*, 104951. [CrossRef] [PubMed]
44. Tian, L.; Yuan, S.; Quiring, S.M. Evaluation of Six Indices for Monitoring Agricultural Drought in the South-Central United States. *Agric. For. Meteorol.* **2018**, *249*, 107–119. [CrossRef]
45. Wu, J. *Agricultural Drought Monitoring and Prediction Using Soil Moisture Deficit Index*; University of North Dakota: Grand Forks, ND, USA, 2014.
46. Vicente-Serrano, S.M.; Quiring, S.M.; Peña-Gallardo, M.; Yuan, S.; Domínguez-Castro, F. A Review of Environmental Droughts: Increased Risk under Global Warming? *Earth-Sci. Rev.* **2020**, *201*, 102953. [CrossRef]
47. Türkeş, M.; Akgündüz, A.S.; Demirörs, Z. Palmer Kuraklık İndisi'ne Göre İç Anadolu Bölgesi'nin Konya Bölümü'ndeki Kurak Dönemler ve Kuraklık Şiddeti. *Coğrafi Bilim. Derg.* **2009**, *7*, 129–144. [CrossRef]
48. Khatiwada, K.R.; Pandey, V.P. Characterization of Hydro-Meteorological Drought in Nepal Himalaya: A Case of Karnali River Basin. *Weather Clim. Extrem.* **2019**, *26*, 100239. [CrossRef]
49. Dai, A. Drought under Global Warming: A Review. *WIREs Clim. Change* **2011**, *2*, 45–65. [CrossRef]
50. Şen, Z. Drought Hazard Mitigation and Risk. In *Applied Drought Modeling, Prediction, and Mitigation*; Elsevier: Amsterdam, The Netherlands, 2015; pp. 393–459. [CrossRef]
51. Yu, M.; Li, Q.; Lu, G.; Wang, H.; Li, P. Development and Application of a Short-/Long-Term Composited Drought Index in the Upper Huaihe River Basin, China. *Proc. Int. Assoc. Hydrol. Sci.* **2015**, *369*, 103–108. [CrossRef]
52. Saxton, K.E.; Rawls, W.J. Soil Water Characteristic Estimates by Texture and Organic Matter for Hydrologic Solutions. *Soil Sci. Soc. Am. J.* **2006**, *70*, 1569–1578. [CrossRef]
53. Hengl, T.; Mendes de Jesus, J.; Heuvelink, G.B.M.; Ruiperez Gonzalez, M.; Kilibarda, M.; Blagotić, A.; Shangguan, W.; Wright, M.N.; Geng, X.; Bauer-Marschallinger, B.; et al. SoilGrids250m: Global Gridded Soil Information Based on Machine Learning. *PLoS ONE* **2017**, *12*, e0169748. [CrossRef] [PubMed]
54. Thornthwaite, C.W. An Approach toward a Rational Classification of Climate. *Geogr. Rev.* **1948**, *38*, 55. [CrossRef] [PubMed]
55. van der Schrier, G.; Jones, P.D.; Briffa, K.R. The sensitivity of the PDSI to the Thornthwaite and Penman-Monteith parameterizations for potential evapotranspiration. *J. Geophys. Res.* **2011**, *116*, D03106. [CrossRef]
56. Hirsch, R.M. A Comparison of Four Streamflow Record Extension Techniques. *Water Resour. Res.* **1982**, *18*, 1081–1088. [CrossRef]
57. Carvalho, D.; Pereira, S.C.; Silva, R.; Rocha, A. Aridity and Desertification in the Mediterranean under EURO-CORDEX Future Climate Change Scenarios. *Clim. Change* **2022**, *174*, 28. [CrossRef]

58. Essa, Y.H.; Hirschi, M.; Thiery, W.; El-Kenawy, A.M.; Yang, C. Drought Characteristics in Mediterranean under Future Climate Change. *npj Clim. Atmos. Sci.* **2023**, *6*, 133. [CrossRef]
59. Çelik, M.A.; Simsek, O.; Akiner, M.E.; Kızılelma, Y. Impacts of Climate Change on Meteorological and Hydrological Drought Dynamics in a Mediterranean Basin: The Case of Göksu River Basin, Türkiye. *Meteorol. Atmos. Phys.* **2026**, *138*, 45. [CrossRef]
60. Mares, C.; Mares, I.; Mihailescu, M. Identification of Extreme Events Using Drought Indices and Their Impact on the Danube Lower Basin Discharge. *Hydrol. Process.* **2016**, *30*, 3839–3854. [CrossRef]
61. Naumann, G.; Dutra, E.; Barbosa, P.; Pappenberger, F.; Wetterhall, F.; Vogt, J.V. Comparison of Drought Indicators Derived from Multiple Data Sets over Africa. *Hydrol. Earth Syst. Sci.* **2014**, *18*, 1625–1640. [CrossRef]
62. Çelik, M.A. A Multi-Method Geospatial Framework for Drought Risk Assessment in the GAP Region (Türkiye): Trend Analysis, Dry-Spell Persistence and Random Forest Forecasting. *Ecohydrology* **2026**, *19*, e70234. [CrossRef]

Disclaimer/Publisher's Note: The statements, opinions and data contained in all publications are solely those of the individual author(s) and contributor(s) and not of MDPI and/or the editor(s). MDPI and/or the editor(s) disclaim responsibility for any injury to people or property resulting from any ideas, methods, instructions or products referred to in the content.